© IWA Publishing 2020
863

Water Practice & Technology Vol 15 No 4
doi: 10.2166/wpt.2020.094

Effects of chemical activating agents on physical properties of activated carbons – a commentary

Fadina Amran[a,b] and Muhammad Abbas Ahmad Zaini[a,b,*]

[a] Centre of Lipids Engineering & Applied Research (CLEAR), Ibnu-Sina Institute for Scientific & Industrial Research (ISI-SIR), Universiti Teknologi Malaysia, 81310 UTM Johor Bahru, Johor, Malaysia

[b] School of Chemical & Energy Engineering, Faculty of Engineering, Universiti Teknologi Malaysia, 81310 UTM Johor Bahru, Johor, Malaysia

*Corresponding author. E-mail: abbas@cheme.utm.my

Abstract

Well-developed surface areas and porous structures that render high adsorption capacity are necessary for pollutant removal from wastewater by activated carbons. Activated carbons from natural resources, and agricultural and industrial waste materials are produced using chemical agents, including KOH, H_3PO_4, K_2CO_3, $ZnCl_2$ and NaOH. This study is intended to highlight the effects of those agents on the physical properties of the activated carbons. The operating conditions, i.e., temperature, time and ratio, show an interplay towards the physical properties at varying degree. The yield, pore size, mesoporosity and surface area of activated carbons derived using different chemical agents correlate well with the impregnation ratio. Generally, the pore size, mesoporosity and surface area increase, while the yield decreases with increasing ratio (over a given range). Higher ratio and temperature are recommended for KOH, K_2CO_3 and NaOH activation, to endow activated carbons with greater surface area.

Key words: activated carbon, activation conditions, chemical activation, correlation, physical properties

Highlights

- Physical properties of activated carbons by different chemical activation strategies.
- H_3PO_4 activation produces higher carbon yield.
- Relationships between activation conditions and physical properties of activated carbons were presented.
- Interplay of activating agents and operating conditions towards excellent physical properties of activated carbon.

INTRODUCTION

Water is the foundation of life. However, the rapid growth of the world's population and poor wastewater management have led to increased wastewater production and associated implications for the environment. Wastewater generally contains suspended solids, dyes, heavy metals and/or salts. According to Sutisna *et al.* (2017), the stability of such materials makes them difficult to degrade. At high concentration, they are harmful to the environment and aquatic ecosystems, as they can raise the chemical oxygen demand of water. Therefore, wastewater is a serious problem that requires effective treatment.

Adsorption is an effective and preferred method to abate water contaminants, even at low concentrations. The process is simple and easy to scale up, is often based on low-cost adsorbents, and produces small quantities of sludge or by-products (Ismail *et al.* 2013; Rangabhashiyam *et al.* 2013;

Water Practice & Technology Vol 15 No 4
doi: 10.2166/wpt.2020.094

Reza & Ahmaruzzaman 2015). Activated carbon (AC), and ion exchange materials such as zeolite and bentonite clay are widely used in adsorption studies. AC is a versatile adsorbent with a large specific surface, highly porous structure, and high adsorption capacity and surface reactivity. Commercial AC is often used to remove water pollutants but can be expensive, so the quest for economical and high performance materials has become a subject of considerable interest. New ACs from different precursors such as natural resources, or agricultural or industrial residues via various activation strategies, have been developed and tested for wastewater treatment.

AC is generally prepared by physical and/or chemical activation. Chemical activation is advantageous in producing ACs with high carbon yield and surface area, and rich surface functional groups for high adsorption capacity. The specific surface usually exceeds 1,000 m^2/g, with 5 g equivalent to a football field (Arvanitoyannis *et al.* 2008). The wide pore size distribution and well-developed pore structure bring about a high specific surface to capture and entrap the target molecules. Pore sizes are classified as micropore (<2 nm), mesopore (between 2 and 50 nm) and macropore (>50 nm). Microporous AC is normally used to adsorb gases and vapours, while the mesoporous material is preferred for larger molecules such as dyes and organic pollutants. A relatively high number of micropores is required for gas adsorption because most gas molecules have diameters below 1.0 nm. On the other hand, plentiful mesopores are necessary for liquid adsorption due to the larger molecular size of water contaminants. Thus, adsorption capacity is influenced significantly by pore size distribution as well as the size of adsorbate molecules.

ACs have been chemically activated from various carbonaceous materials. However, there is still limited literature on the effects of the chemical activators associated with various activation parameters and the physical properties of the ACs. The aim of this study is to summarise and correlate the activation parameters (temperature, time, ratio) with the ACs' physical properties to give deeper insight into the possible interactions between the chemical agents and carbon materials.

CHEMICAL ACTIVATION – AN OVERVIEW

AC production has two steps: carbonization and activation. Carbonization is pyrolysis of the material at high temperature (500 to 1,000 °C) in an inert atmosphere. The aim is to liberate tar, hydrocarbons and volatiles to enrich the carbon content, at the same time creating an initial char porosity (Ma *et al.* 2017). Activation has significant effects on the AC matrix, especially in the formation of the pore structure, giving rise to a high specific surface. AC can be produced from a variety of carbonaceous materials by physical and/or chemical activation.

Physical char activation is performed using steam and/or carbon dioxide as the oxidising gas. Porosity is developed by controlling gasification of the carbon material. Carbon dioxide has low reactivity and is preferable to steam to develop uniform porosity by regulating the oxidation rate (Contescu *et al.* 2018). The activation temperature is normally in the range of 600 to 1,000 °C (Nandi *et al.* 2012; Guan *et al.* 2013; Ghouma *et al.* 2015). Unlike chemical activation, this process has no chemical mixing; it is preferable in term of environmental safety, but requires high operating temperature and often results in low product yield (Yang *et al.* 2010; Zhou *et al.* 2018).

Chemical activation is a single-step process where carbonization and activation happen simultaneously. In several cases, a pre-carbonization step is introduced to produce char prior to chemical impregnation and activation (Fu *et al.* 2019; Sangachini *et al.* 2019; Yang *et al.* 2019). Undergoing pre-carbonization enables initial pore development with a greater specific surface on activation (Zaini & Kamaruddin 2013). Two-step activation allows more activating agent to react with the carbon compound, yielding greater pore volume and a larger AC specific surface (Saad *et al.* 2019).

Chemical activation is more advantageous than physical activation because it produces higher carbon yield, rich in micro- and meso-pores with better specific surface and adsorption capacity.

Water Practice & Technology Vol 15 No 4
doi: 10.2166/wpt.2020.094

The chemical agents possess dehydrogenation properties to inhibit tar formation and avoid excessive volatile production to give high carbon yields (Zhang *et al.* 2008). It usually requires lower activation temperature (400 to 800 °C) and shorter activation time (30 minutes to 3 hours), depending on the raw materials and activating agents used (Zhang *et al.* 2010; Gumus & Okpeku 2015; Borhan *et al.* 2018). At high temperatures and with prolonged activation, the pore walls tend to collapse due to sintering and realignment of the carbon structure, thus decreasing the pore characteristics and specific surface needed for efficient adsorbent-adsorbate interactions (Hock & Zaini 2018).

STRATEGIES IN CHEMICAL ACTIVATION

Selection of the ratio of the chemical agent to precursor is important for producing an AC with good yield, specific surface and adsorption properties. Typical values are in the range 0.5 to 3 (Tang & Zaini 2016; Astuti *et al.* 2019; Sangachini *et al.* 2019). Activating agents oxidise a weak part of the carbon matrix to generate pores. A large agent:precursor ratio often results in a limited specific surface because of collapse of the pore structure, although a high ratio that produces a high specific surface could arise from high molecular weight precursor material, which could minimise the loss.

Alkali and alkaline earth metals, and some acids, are normally used as activating agents. Examples include potassium hydroxide (KOH) (Fu *et al.* 2019; Seo *et al.* 2019; Yang *et al.* 2019), phosphoric acid (H_3PO_4) (Kang *et al.* 2018; Wu *et al.* 2018; Baek *et al.* 2019), potassium carbonate (K_2CO_3) (Zhou *et al.* 2012; Garba *et al.* 2015; Oliveira *et al.* 2018), zinc chloride ($ZnCl_2$) (Vunain *et al.* 2018; Laverde *et al.* 2019; Ma *et al.* 2019) and sodium hydroxide (NaOH) (Laverde *et al.* 2019; Hasanzadeh *et al.* 2020; Zhang *et al.* 2020).

Hydroxides like KOH and NaOH have been used widely to produce ACs with well-developed porosity and high specific surface. However, KOH is poisonous, and toxic to humans and aquatic creatures, so its role as a chemical agent should be considered carefully in relation to environmental sustainability. According to Hui & Zaini (2015), KOH is not completely vaporized in the impregnated precursor, as the activation temperature is generally below its boiling point (1,327 °C). Hence, the washing step must allow for the recovery of spent KOH to prevent its release to the environment. In comparison, NaOH is cheaper, more environmentally friendly and less harmful than KOH. K_2CO_3 is also non-hazardous and brings fewer adverse effects from activation.

H_3PO_4 is relatively non-polluting in character compared to $ZnCl_2$. ACs produced by H_3PO_4 activation are typically used to remove colour or organic pollutants from water. $ZnCl_2$, like KOH, is toxic and requires additional measures to recover the spent agent for subsequent use in activation. H_3PO_4 activation (375 to 500 °C) always causes corrosion in steel equipment, while zinc deposits in $ZnCl_2$ ACs (550 to 650 °C) are difficult to remove (Buczek 2016). Tables 1–5 summarise the preparation and properties of ACs using KOH, H_3PO_4, K_2CO_3, $ZnCl_2$ and NaOH, respectively. The ratio is given as the chemical agent to precursor.

RELATIONSHIPS BETWEEN ACTIVATION STRATEGIES AND PHYSICAL PROPERTIES OF ACS

Table 1 shows the properties of KOH-activated ACs. These have specific surfaces in the range of 285 to 3,230 m^2/g. Using operating conditions comprising ratio 1.5, 800 °C and 1 hour yields an AC with 285 m^2/g specific surface (Yang *et al.* 2019), while 3,230 m^2/g is achieved with ratio 4, 800 °C and 1 hour (Seo *et al.* 2019). Further comparison has been made because both precursors have carbon content >50% (Seo *et al.* 2019; Yang *et al.* 2019). In general, as the ratio is increased, more of the chemical agent can move into the carbon matrix, increasing pore development during activation, thus boosting the specific surface. Above some upper threshold, however, the precursor's structural

Water Practice & Technology Vol 15 No 4
doi: 10.2166/wpt.2020.094

Table 1 | Preparation and properties of KOH ACs

Material	Activation strategies (ratio, temp, time)	Yield (%)	Specific surface (m^2/g)	Mesoporosity (%)	Pore size (nm)	Adsorption pollutant model	Reference
Petroleum-based pitch	1:1, 800 °C, 1 h	76.8	1,280	–	1.3	Argon	Seo *et al.* (2019)
Petroleum-free pitches		67.2	1,160	–	1.3		
Petroleum-based pitch	2:1, 800 °C, 1 h	70.4	2,170	–	1.4		
Petroleum-free pitches		63.6	2,230	–	1.4		
Petroleum-based pitch	4:1, 800 °C, 1 h	59.3	3,230	–	1.8		
Petroleum-free pitches		61.6	1,960	–	1.5		
Rice husk	1:1, 750 °C, 3 h Pre-carbonisation: 450 °C, 3 h Activation: 1:1, 750 °C, 1 h	2.5 19.4	589 741	57.6 33.3	2.14 1.98	Phenol	Fu *et al.* (2019)
Rice husk	Pre-carbonisation: 450 °C, 3 h	–	133	85.7	1.43	Phenol	Shen *et al.* (2019)
Rice husk pellets		–	173	87.5	1.33		
Rice husk	1:1, 750 °C, 1 h	–	779	71.8	1.85		
Rice husk pellets		–	859	83.7	1.33		
Rice husk	3:1, 750 °C, 1 h	–	1,818	93.3	1.20		
Rice husk pellets		–	1,320	69.2	1.62		
Municipal sewage sludge and coconut shell	1.5:1, 800 °C, 1 h Pre-carbonisation: 500 °C, 45 min Activation: 1.5:1, 800 °C, 1 h	– –	285 684	54 72	4.47 3.79	Methylene blue	Yang *et al.* (2019)
Walnut shell	Pre-carbonisation: 600 °C, 1.5 h Activation: 1.5:1, 900 °C, 2.5 h	–	728	94	1.38	CO_2	Sangachini *et al.* (2019)
Arundo donax	1:1, 600 °C, 2 h 2:1, 600 °C, 2 h	– –	637 1,122	72 84	0.56 0.56	CO_2	Singh *et al.* (2017)
Rice husk	Pre-carbonisation: 450 °C, 3 h 1:1, 750 °C, 1 h 3:1, 750 °C, 1 h	– – –	133 779 1,818	14.3 15.3 12.2	1.43 1.85 1.20	Toluene and phenol	Shen & Zhang (2019)
Wood residue (white birch)	Pre-carbonisation: 800 °C, 2 Activation: 3:1, 900 °C, 2 h	–	1,700	100	–	Copper	Braghiroli *et al.* (2019)
Wood residue (black spruce)		–	1,662	100	–		
Polyacrylonitrile (PAN)	Pre-carbonisation: 800 °C, 2 h Activation: 1:1, 800 °C, 2 h	–	1,156	48.5	–	CO_2	Singh *et al.* (2019)
	Pre-carbonisation: 800 °C, 2 h Activation: 3:1, 800 °C, 2 h	–	1,884	31.3	–		

stability is inadequate and the pores tend to collapse. Similarly, increasing the chemical ratio produces a positive trend in mesoporosity and pore size (Singh *et al.* 2017; Seo *et al.* 2019; Shen & Zhang 2019). Use of large amounts of KOH damages the carbon walls, yielding a continuous pore structure, and increases the pore size and volume, as well as the specific surface, by oxidation and gasification at high temperature. Carbon gasification rates can also be improved to promote pore formation, although mesoporosity may decrease because excess pore widening destroys mesopores (Shen *et al.* 2019; Singh *et al.* 2019).

Water Practice & Technology Vol 15 No 4
doi: 10.2166/wpt.2020.094

Table 2 | Preparation and properties of H_3PO_4 ACs

Material	Activation strategies (ratio, temp, time)	Yield (%)	Specific surface (m^2/g)	Mesoporosity (%)	Pore size (nm)	Adsorption pollutant model	Reference
Cotton stalk (*Gossypium hirsutum* L.)	0.3:1, 500 °C, 2 h	56.8	330	6.25	3.4	–	Nahil & Williams (2012)
	0.75:1, 500 °C, 2 h	55.4	1,200	11.5	3.4	–	
	1.5:1, 500 °C, 2 h	53.7	1,720	20.2	3.4	–	
Peach stone	0.22:1, 500 °C, 2 h	42.6	1,153	–	1.0	Methylene blue	Attia *et al.* (2008)
	0.43:1, 500 °C, 2 h	41.8	1,393	–	0.99		
	1:1, 500 °C, 2 h	43.8	1,153	–	0.99		
Globe artichoke leaf	1:1, 500 °C, 1 h	37	1,745	37.5	2.9	Methylene blue	Benadjemia *et al.* (2011)
	2:1, 500 °C, 1 h	25	2,038	73.0	3.0		
	3:1, 500 °C, 1 h	31	1,607	73.9	3.0		
Humin	6.7:1, 300 °C, 2 h	73.5	1,358	–	–	Methylene blue	Kang *et al.* (2018)
	6.7:1, 400 °C, 2 h	51.4	2,375	–	1.97		
	6.7:1, 600 °C, 2 h	55.0	1,774	–	–		
Bacterial cellulose	1:1, 400 °C, 1 h	40.2	1,540	–	2.25	Methylene blue	Khamkeaw *et al.* (2018)
	1:1, 500 °C, 1 h	33.4	1,734	–	2.33		
	1:1, 600 °C, 1 h	26.4	1,702	–	2.37		
Kenaf stem	1:1, 600 °C, 1.5 h	43	610	47.4	2.48	–	Baek *et al.* (2019)
	2:1, 600 °C, 1.5 h	45	1,020	56.8	3.15	–	
	3:1, 600 °C, 1.5 h	37	1,570	70.3	4.63	–	
Peanut shell	Pre-carbonisation: 450 °C, 3 h	–	591	22.0	1.83	Reactive brilliant blue X- BR	Wu *et al.* (2018)
	3:1, 450 °C, 3 h	–	1,138	30.0	2.34		

Table 3 | Preparation and properties of K_2CO_3 ACs

Material	Activation strategies (ratio, temp, time)	Yield (%)	Specific surface (m^2/g)	Mesoporosity (%)	Pore size (nm)	Adsorption pollutant model	Reference
Brachystegia eurycoma seed hull	1:1, 760 °C, 2 h	19.2	1,218	–	3.25	Malachite green	Garba *et al.* (2015)
Palm shell	2:1, 700 °C, 2 h	22.2	425	–	0.72	–	Adinata *et al.* (2007)
	2:1, 800 °C, 2 h	18.9	1,170	–	0.73	–	
	2:1, 900 °C, 2 h	16.8	544	–	0.75	–	
Palm shell	Pre-carbonisation: 450 °C, 1 h	36	815	43.1	2.85	Methylene blue	Hao & Xianlun (2013)
	1:2, 850 °C, 1 h	30	982	38.5	1.65		
Paper pulp (bleached pulp)	Pre-carbonisation: 800 °C, 2.5 h	25	3	66.7	7.9	Pharmaceuticals (anti-epileptic carbamazepine and antibiotic sulfamethoxazole)	Oliveira *et al.* (2018)
Paper pulp (raw pulp)		18	5	100	9.43		
Paper pulp (bleached pulp)	1:1, 800 °C, 2.5 h	5	855	72.3	2.69		
Paper pulp (raw pulp)		4	814	73.2	2.66		
Lentil waste	1:1, 800 °C, 1 h	–	1,253	55.3	1.85	Methylene blue and Methyl orange	Saygili & Saygili (2019)
	2:1, 800 °C, 1 h	–	1,563	83.2	2.21		
	3:1, 800 °C, 1 h	38	1,875	63.9	1.97		
Oxytetracycline bacterial residue	1:1, 800 °C, 3 h	–	874	29	3.16	Phenol	Zhou *et al.* (2012)
	2:1, 800 °C, 3 h	–	1,084	29.6	2.62		
	3:1, 800 °C, 3 h	–	1,593	31.0	2.18		

Water Practice & Technology Vol 15 No 4
doi: 10.2166/wpt.2020.094

Table 4 | Preparation and properties of $ZnCl_2$ ACs

Material	Activation strategies (ratio, temp, time)	Yield (%)	Specific surface (m^2/g)	Mesoporosity (%)	Pore size (nm)	Adsorption pollutant model	Reference
Liquefied wood	Pre-carbonisation: 700 °C, 1 h Activation: 3:1, 700 °C, 1 h	44.4	762	42.8	13.3	Methylene blue	Ma *et al.* (2019)
	3:1, 700 °C, 1 h	53.8	1,086	59.4	13.3		
Sunflower (*Helianthus annuus*) seed hull	Pre-carbonisation: 800 °C, 1 h	24.9	206	21.3	1.65	Catechol and resorcinol	Vunain *et al.* (2018)
	1.5:1, 800 °C, 1 h	73.6	1,374	3.34	1.92		
Guava seed	Pre-carbonisation: 300 °C, 1 h Activation: 3:1, 500 °C, 2 h	24.0	919	–	2.37	2,4-dichlorophenol	Anisuzzaman *et al.* (2016)
Oil palm shell	Pre-carbonisation: 300 °C, 1 h Activation: 4:1, 500 °C, 2 h	56.8	1,020	–	2.44	Phenol	Anisuzzaman *et al.* (2018)
Rice husk	3:1, 500 °C, 1 h	33.1	138	100	3.04	Acetaminophen	Laverde *et al.* (2019)
Coffee husk		51.4	613	41.4	1.91		
Fox nutshell (*Euryale ferox*)	1:1 600 °C, 1 h	42.0	1,601	4.49	2.22	–	Kumar & Jena (2015)
	1.5:1 600 °C, 1 h	37.5	2,028	5.08	2.32	–	
	2:1 600 °C, 1 h	33.0	2,869	14.3	2.73	–	
Mangosteen peel	2:1, 600 °C, 30 min	–	1,128	84.0	2.22	Methylene blue	Nasrullah *et al.* (2018)
	4:1, 600 °C, 30 min	51.9	1,622	100	4.85		
	6:1, 600 °C, 30 min	–	1,115	96.0	4.47		
Sugar cane bagasse	3:1, 500 °C, 2 h	–	1,145	88.5	2.65	Diclofenac sodium	Naga *et al.* (2019)
Capparis scabrida sawdust	1:1, 600 °C, 2 h	–	1,676	21.8	3.75	Tartrazine, Brilliant scarlet 4R, Brilliant blue	Valladares *et al.* (2019)
Aegle marmelos fruit shell	0.5:1, 500 °C, 2 h	–	346	3.68	0.78	Chromium (VI)	Gottipati & Mishra (2016)
	1:1, 500 °C, 2 h	–	592	5.18	1.87		
	2:1, 500 °C, 2 h	–	872	10.0	2.95		
Peanut shell	5:1, 480 °C, 2 h	–	1,025	25.1	0.70	Toluene, ethyl benzene	Bedane *et al.* (2018)

Generally, direct chemical activation is less effective than two-step activation because the former is concentrated mainly on the carbon surface and the interior matrix does not react with the agent. Too low an activation temperature could result in less polymerization, with more carbon atoms escaping in gases. Precursors that have been pre-carbonised have undergone condensation and rearrangement reaction, releasing gases and then forming amorphous structures with preliminary porosity. The resulting specific surface for direct and two-step KOH activation increased from 589 to 741 m^2/g (Fu *et al.* 2019). Similarly, KOH-activated municipal sludge mixed with coconut shell shows a specific surface increase from 285 to 684 m^2/g (Yang *et al.* 2019). During activation, the activator promoted pore formation and/or enlargement of small pores within the carbon matrix. Most KOH-activated ACs demonstrate good mesoporosity and pore size development, but the yield is relatively low probably due to KOH's dehydrating effect (around 2.5 to 24.3%).

Water Practice & Technology Vol 15 No 4
doi: 10.2166/wpt.2020.094

Table 5 | Preparation and properties of NaOH ACs

Material	Activation strategies (ratio, temp, time)	Yield (%)	Specific surface (m^2/g)	Mesoporosity (%)	Pore size (nm)	Adsorption pollutant model	Reference
Rice husk	Pre-carbonisation: 500 °C, 1 h Activation: 3:1, 800 °C, 1.5 h	14.3	2,786	8.44	2.40	Lead ions	Zhang *et al.* (2020)
Soybean shell	Pre-carbonization: 500 °C, 1 h Activation: 4:1, 800 °C, 1.5 h	10.2	2,628	9.95	2.60		
Date press cake	Pre-carbonisation: 500 °C, 2 h Activation: 3:1, 700 °C, 1.5 h	26.0	2,623	22.3	2.04	Cefixime	Hasanzadeh *et al.* (2020)
Rice husk	Pre-carbonisation: 500 °C, 2 h Activation: 3:1, 500 °C, 1 h	59.3	626	65.7	2.20	Acetaminophen	Laverde *et al.* (2019)
	Pre-carbonisation: 500 °C, 2 h Activation: 3:1, 650 °C, 1 h	57.1	709	43.4	2.19		
	Pre-carbonisation: 500 °C, 2 h Activation: 3:1, 800 °C, 1 h	56.6	1,004	31.5	2.13		
Argan hard shell	Pre-carbonisation: 700 °C, 1 h Activation: 4:1, 850 °C, 1 h	–	1,827	76.0	3.00	CO_2	Boujibar *et al.* (2018)
Tofu	2:1, 800 °C, 2 h	–	1,143	37.5	3.25	–	Lei *et al.* (2019)
Coconut coir pith	Pre-carbonisation: 650 °C, 2 h Activation: 1:1, 700 °C, 1 h	28.5	633	15.4	1.30	–	Sesuk *et al.* (2019)
	Pre-carbonisation: 650 °C, 2 h Activation: 2:1, 700 °C, 1 h	27.4	860	13.7	1.30	–	
	Pre-carbonisation: 650 °C, 2 h Activation: 3:1, 700 °C, 1 h	26.3	2,056	9.40	1.30	–	

Table 2 shows the properties of H_3PO_4-activated ACs. These are reported with specific surfaces ranging from 330 to 2,375 m^2/g and pore sizes from 2.33 to 4.63 nm, suitable for large adsorbate molecules. ACs show increases in mesoporosity, pore size and specific surface with increasing ratio, but the yield decreases (Nahil & Williams 2012; Baek *et al.* 2019). H_3PO_4-activated humin has a high specific surface of 2,375 m^2/g and the yield was 51.4% (Kang *et al.* 2018). H_3PO_4 promotes bond cleavage and crosslink formation; the phosphate groups enhance pore formation in an expanded state on the carbon material. Its use could limit damage to the humin structure, with a high AC yield. There are also reports of decreasing specific surface and yield as the activation ratio and temperature increase (Attia *et al.* 2008; Benadjemia *et al.* 2011; Kang *et al.* 2018; Khamkeaw *et al.* 2018). H_3PO_4 loses water at temperatures above 300 °C, potentially leading to pore destruction

Water Practice & Technology Vol 15 No 4
doi: 10.2166/wpt.2020.094

due to poor resistance to acid catalytic activity. Pore blockage and shrinkage, and partial collapse of the carbon structure could also occur, leading to decreased pore volume and specific surface.

Table 3 summarises the properties of K_2CO_3-activated ACs. The specific surfaces of these is significantly smaller than those from other activators. K_2CO_3-activated lentil waste produced with ratio 3, 800 °C, 1 hour has 1,875 m^2/g specific surface and 38% yield (Saygili & Saygili 2019). The specific surface increased as the ratio was increased from 1 to 3 (Zhou *et al.* 2012; Saygili & Saygili 2019), but fell as the temperature was increased from 700 to 900 °C (Adinata *et al.* 2007). Potassium from K_2CO_3 reduction diffuses into the inner carbon structure, widening the existing pores to increase the pore volume. However, too high a temperature increases the carbon-K_2CO_3 reaction rate, resulting in increasing carbon burn-off and decreasing specific surface. Oliveira *et al.* (2018) reported 100% mesoporosity of AC from pre-carbonised paper pulp at 800 °C and 2.5 h, which implies that the char released more volatiles and had a high potential for porosity development despite the lower specific surface. The literature for this activator is limited because it does not work well in AC production and offers low yields (4 to 5%).

Table 4 shows the properties of $ZnCl_2$-ACs. A specific surface of 2,869 m^2/g was recorded for $ZnCl_2$-activated fox nutshell at ratio 2, 600 °C and 1 hour (Kumar & Jena 2015). The specific surface, mesoporosity and pore size increased as the ratio was increased from 0.5 to 2 (Kumar & Jena 2015; Gottipati & Mishra 2016). The trend changed as the ratio was increased to 6 (Nasrullah *et al.* 2018). Generally, $ZnCl_2$ activation causes the cellulose molecular structure to swell, breaking lateral bonds in cellulose molecules, and increases the inter- and intra-micelle voids for higher specific surface. A high ratio amplifies the collapse of existing pores within the carbon matrix. Accordingly, two-stage $ZnCl_2$ activation reduced pore size, specific surface and yield relative to direct activation (Ma *et al.* 2019). Carbonisation and activation occurred simultaneously on the carbon material at optimum temperature to produce a relatively stable carbon structure, with lower incidence of volatiles and by-products.

Table 5 shows the properties of NaOH-activated ACs. Rice husk-based, pre-carbonised AC has a 2,786 m^2/g specific surface but relatively low 14.3% yield (Zhang *et al.* 2020). However, Laverde *et al.* (2019) reported a specific surface of 1,004 m^2/g for the same material and conditions apart from 0.5 hour activation time. High mesoporosity implies that micropores merge into mesopores during pore formation, reducing the number of active sites and specific surface. Varying the impregnation ratio from 1 to 3 increased the specific surface from 633 to 2,056 m^2/g (Sesuk *et al.* 2019).

Figures 1–5 illustrate the correlation between the AC activation parameters (temperature, time, ratio) and their physical properties. The figures are arbitrarily plotted from data in Tables 1–5.

As can be seen in Figure 1, there is a positive correlation between AC properties and KOH ratio. The regression line for activation conditions of 500 to 600 °C for 1 to 2 hours is steeper than that of 700 to 800 °C, 1 to 2 hours, implying that a high ratio would be required to produce an AC rich in mesopore content and surface area. A temperature of 700 to 800 °C for 1 to 2 hours is also recommended because the properties of ACs produced under these conditions are better, assuming that all carbonaceous materials have the same characteristics. In many published works related to AC production, carbonaceous materials with high carbon content – of between 40 and 60% – are often used in chemical activation (Singh *et al.* 2017; Braghiroli *et al.* 2019; Singh *et al.* 2019).

H_3PO_4 activation requires temperatures in the range 300 to 600 °C. The conditions show good correlation with the AC properties, except for yield. ACs derived at 401 to 500 °C show a rising property trend as the ratio increases from 1 to 3. However, the mesoporosity and specific surface decrease as the time is increased to 2 to 3 hours for the same ratio. The negative linear regression of yield versus ratio in Figure 2(a) arises because high ratios accelerate pore development, resulting in carbon loss and lower yield. However, the 31% yield for ratio 3 is still acceptable.

Water Practice & Technology Vol 15 No 4
doi: 10.2166/wpt.2020.094

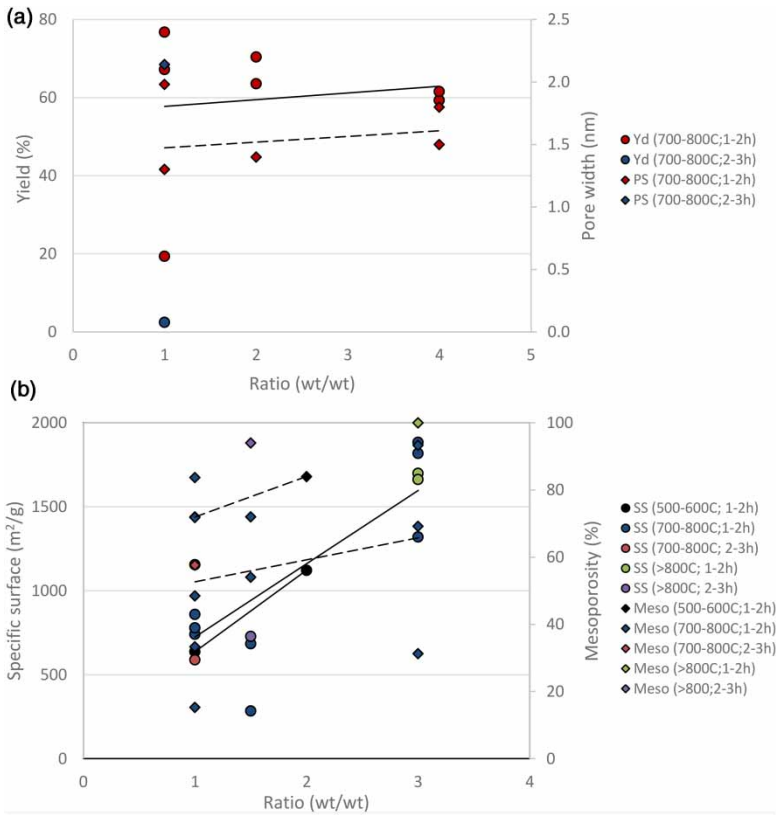

Figure 1 | Effects of KOH activation on AC properties; (a) yield and pore size, and (b) specific surface and mesoporosity.

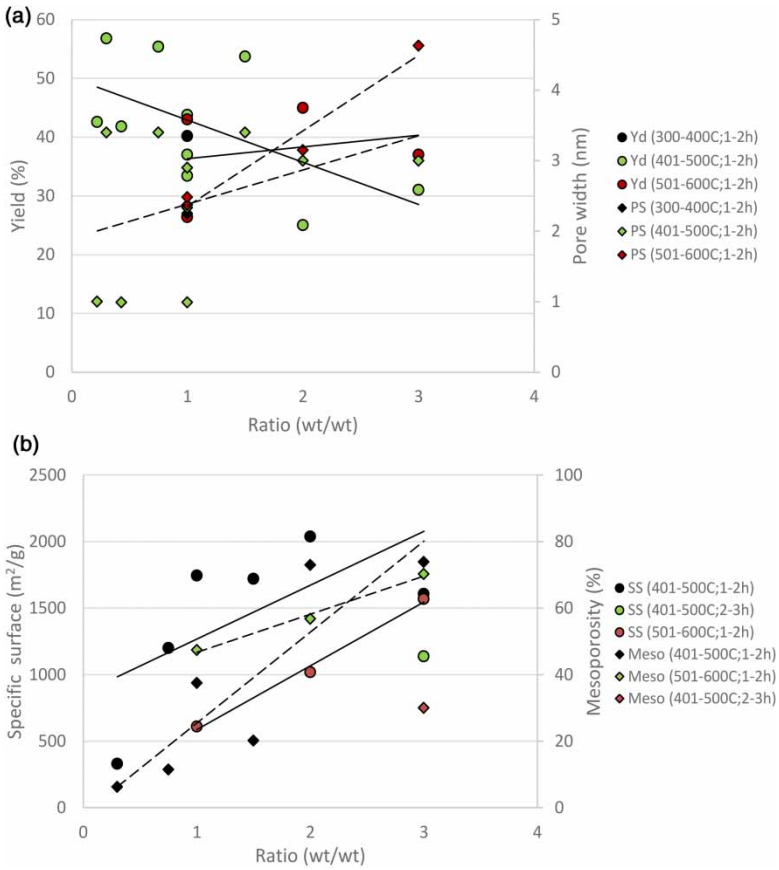

Figure 2 | Effects of H_3PO_4 activation on AC properties; (a) yield and pore size, and (b) specific surface and mesoporosity.

Water Practice & Technology Vol 15 No 4
doi: 10.2166/wpt.2020.094

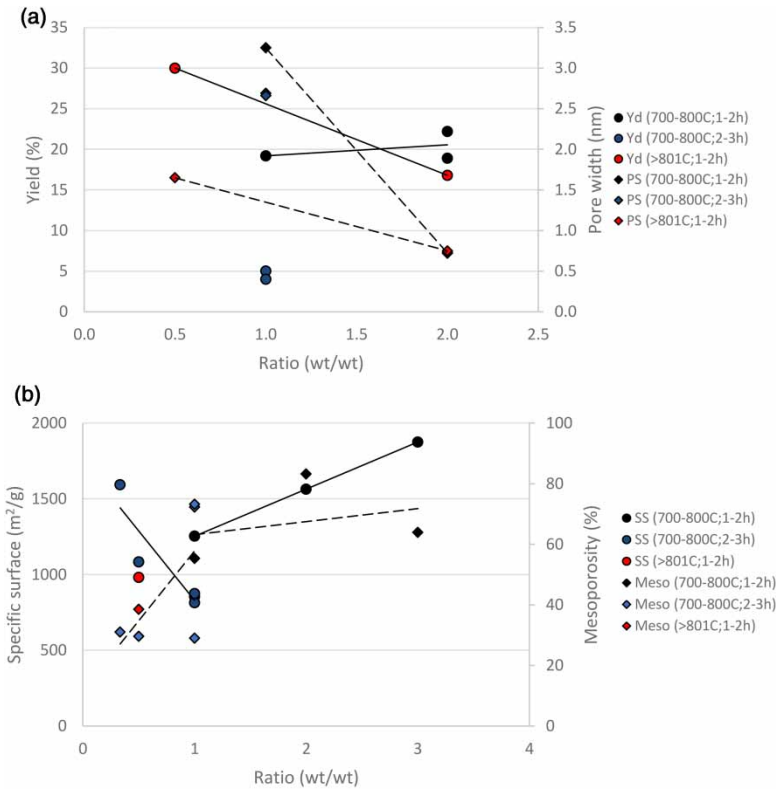

Figure 3 | Effects of K_2CO_3 activation on AC properties; (a) yield and pore size, and (b) specific surface and mesoporosity.

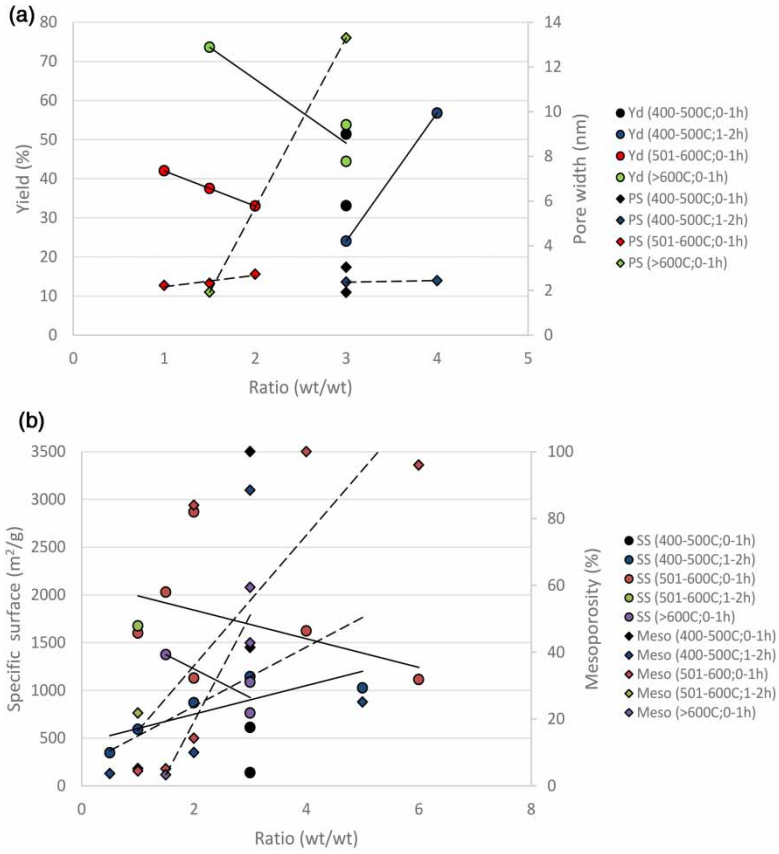

Figure 4 | Effects of $ZnCl_2$ activation on AC properties; (a) yield and pore size, and (b) specific surface area and mesoporosity.

Water Practice & Technology Vol 15 No 4
doi: 10.2166/wpt.2020.094

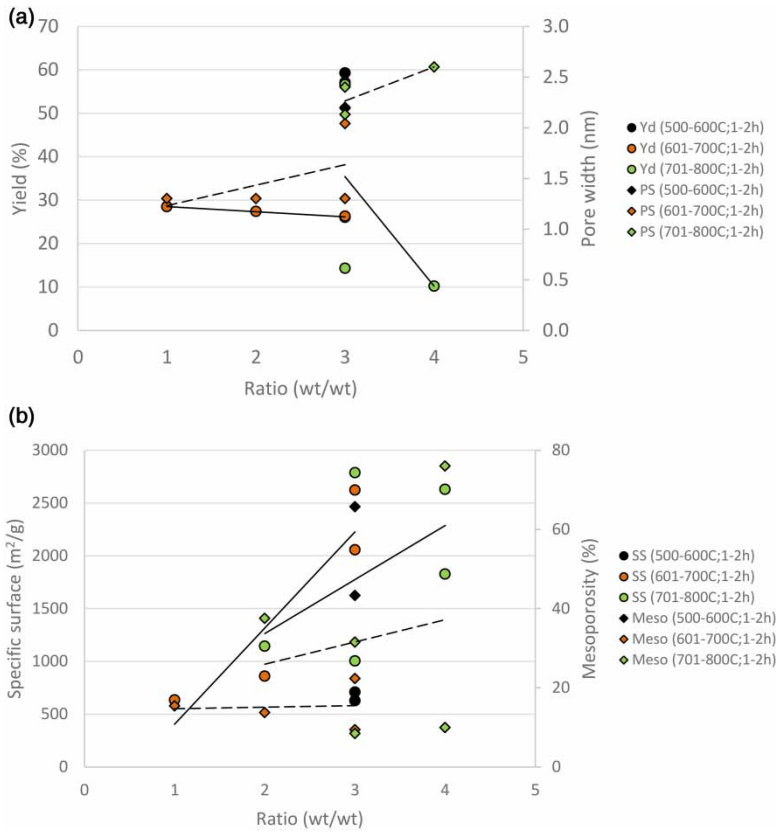

Figure 5 | Effects of NaOH activation on AC properties; (a) yield and pore size, and (b) specific surface area and mesoporosity.

Figure 3(a) shows negative linear regression for K_2CO_3 activation at 700 to 800 °C for 1 to 2 hours. For 1 to 2 and 2 to 3 hours' activation (same ratio and temperature), the yield and pore size are 19% and 33 nm, and 5% and 27 nm, respectively. For ratios in the range of 0.5 to 2.0, there was a significant decrease as activation time and temperature increased. This could suggest that the yield and pore size would be below 5% and 0.5 nm, respectively, for ratio 3. However, the mesoporosity and specific surface (up to 1,875 m^2/g) increase as the ratio increases from 1 to 3. The specific surface at 700 to 800 °C for 2 to 3 hours decreased from 1,400 to 800 m^2/g; despite this, the extended time is recommended as it improves the mesoporosity of K_2CO_3-AC at low impregnation ratios.

Figure 4 shows the relationships between $ZnCl_2$ activation conditions and AC properties. The yield fell from 73.6 to 44.4%, while pore size increased from 1.92 to 13.3 nm as the ratio increased from 1.5 to 3 at >600 °C for 0 to 1 hour. Similarly, activation at 501 to 600 °C for 0 to 1 hour showed the same trend as the ratio increased from 1 to 2. Both activation series exhibit a decline in specific surface with respect to ratio, as shown in Figure 4(b). However, the mesoporosity increased at all activation conditions of ratio 1.5 to 3, >600 °C for 0 to 1 hour, with linear correlation. $ZnCl_2$ activation should be done at a suitable temperature (400 to 600 °C) and time (1 to 2 hours); adequate time gives better swelling, which breaks lateral bonds in carbon material, thus maximizing the formation of inter- and intrapores for a higher specific surface.

The falling trend of yield for conditions of 601 to 700 °C for 1 to 2 hours – Figure 5(a) – could be correlated with ratio, the gradient increasing with temperature. However, the mesopores – from 2.4 to 2.6 nm – are developed much better at higher temperature and ratio. NaOH activation generates about 14% mesoporosity quite consistently, while the specific surface increases from 633 to 2,623 m^2/g (see Figure 5(b)). NaOH activation conditions of 701 to 800 °C for 1 to 2 hours at high ratio are suggested as yielding ACs with greater pore size, rich mesoporosity and high specific surfaces.

Water Practice & Technology Vol 15 No 4
doi: 10.2166/wpt.2020.094

CONCLUSIONS

The physical properties of ACs activated with different chemical agents – that is, KOH, H_3PO_4, K_2CO_3, $ZnCl_2$ and NaOH – are summarised, and the correlations between activation conditions (temperature, time and ratio) and physical properties presented. Linear regression shows that the activation ratio generally correlates well with yield, pore size, mesoporosity and specific surface. Pore size, mesoporosity and specific surface increased, while yield decreased with increasing ratio from 0.5 to 3. The optimum temperature depends, however, on the chemical agent used: 700 °C and above could be recommended for KOH, K_2CO_3, and NaOH, with activation time in the range of 1 to 2 hours.

ACKNOWLEDGEMENTS

This work was funded by Universiti Teknologi Malaysia through SHINE Signature Grant No. 07G80.

DATA AVAILABILITY STATEMENT

All relevant data are included in the paper or its Supplementary Information.

REFERENCES

Adinata, D., Daud, W. M. A. W. & Aroua, M. K. 2007 Preparation and characterization of activated carbon from palm shell by chemical activation with K_2CO_3. *Bioresource Technology* **98**(1), 145–149.

Anisuzzaman, S. M., Joseph, C. G., Krishnaiah, D., Bono, A., Suali, E., Abang, S. & Fai, L. M. 2016 Removal of chlorinated phenol from aqueous media by guava seed (*Psidium guajava*) tailored activated carbon. *Water Resources and Industry* **16**, 29–36.

Anisuzzaman, S. M., Joseph, C. G., Krishnaiah, D., Daud, W. M. A. W., Suali, E. & Chee, F. C. 2018 Sorption potential of oil palm shell for the removal of chlorinated phenol from aqueous solution: kinetic investigation. *Journal of Engineering Science and Technology* **13**(2), 489–504.

Arvanitoyannis, I. S., Kassaveti, A. & Ladas, D. 2008 Food waste treatment methodologies. In: *Waste Management for the Food Industries*, 1st edn (Arvanitoyannis, I. S. ed.). Elsevier Inc., Amsterdam, the Netherlands, pp. 345–410.

Astuti, W., Sulistyaningsih, T., Kusumastuti, E., Thomas, G. Y. R. S. & Kusnadi, R. Y. 2019 Thermal conversion of pineapple crown leaf waste to magnetized activated carbon for dye removal. *Bioresource Technology* **287**, 121426.

Attia, A. A., Girgis, B. S. & Fathy, N. A. 2008 Removal of methylene blue by carbons derived from peach stones by H_3PO_4 activation: batch and column studies. *Dyes and Pigments* **76**(1), 282–289.

Baek, J., Lee, H. M., An, K. H. & Kim, B. J. 2019 Preparation and characterization of highly mesoporous activated short carbon fibers from kenaf precursors. *Carbon Letters* **29**(4), 393–399.

Bedane, A. H., Guo, T. X., Eic, M. & Xiao, H. 2018 Adsorption of volatile organic compounds on peanut shell activated carbon. *Canadian Journal of Chemical Engineering* **97**(1), 238–246.

Benadjemia, M., Milliere, L., Reinert, L., Benderdouche, N. & Duclaux, L. 2011 Preparation, characterization and Methylene Blue adsorption of phosphoric acid activated carbons from globe artichoke leaves. *Fuel Processing Technology* **92**(6), 1203–1212.

Borhan, A., Yit, T. Y., Yusup, S. & Yunus, N. M. 2018 Monoethanolamine wastewater treatment via adsorption using wood sawdust based activated carbon. *Malaysian Journal of Analytical Sciences* **22**(3), 532–541.

Boujibar, O., Souikny, A., Ghamouss, F., Achak, O., Dahbi, M. & Chafik, T. 2018 CO_2 capture using N-containing nanoporous activated carbon obtained from argan fruit shells. *Journal of Environmental Chemical Engineering* **6**(2), 1995–2002.

Braghiroli, F. L., Bouafif, H., Neculita, C. M. & Koubaa, A. 2019 Performance of physically and chemically activated biochars in copper removal from contaminated mine effluents. *Water, Air & Soil Pollution* **230**, 178–192.

Buczek, B. 2016 Preparation of active carbon by additional activation with potassium hydroxide and characterization of their properties. *Advances in Materials Science and Engineering* **2016**, 5819208.

Contescu, C. I., Adhikari, S. P., Gallego, N. C., Evans, N. D. & Biss, B. E. 2018 Activated carbons derived from high-temperature pyrolysis of lignocellulosic biomass. *Journal of Carbon Research* **4**, 4030051.

Fu, Y., Shen, Y., Zhang, Z., Ge, X. & Chen, M. 2019 Activated bio-chars derived from rice husk via one- and two-step KOH-catalyzed pyrolysis for phenol adsorption. *Science of the Total Environment* **646**, 1567–1577.

Water Practice & Technology Vol 15 No 4
doi: 10.2166/wpt.2020.094

Garba, Z. N., Rahim, A. A. & Bello, B. Z. 2015 Optimization of preparation conditions for activated carbon from *Brachystegia eurycoma* seed hulls: a new precursor using central composite design. *Journal of Environmental Chemical Engineering* **3**(4), 2892–2899.

Ghouma, I., Jeguirim, M., Dorge, S., Limousy, L., Ghimbeu, C. M. & Ouederni, A. 2015 Activated carbon prepared by physical activation of olive stones for the removal of NO_2 at ambient temperature. *Comptes Rendus Chimie* **18**(1), 63–74.

Gottipati, R. & Mishra, S. 2016 Preparation of microporous activated carbon from *Aegle Marmelos* fruit shell and its application in removal of chromium (VI) from aqueous phase. *Journal of Industrial and Engineering Chemistry* **36**, 355–363.

Guan, B. T. H., Latif, P. A. & Yap, T. Y. H. 2013 Physical preparation of activated carbon from sugarcane bagasse and corn husk and its physical and chemical characteristics. *International Journal of Engineering Research and Science & Technology* **2**(3), 1–16.

Gumus, R. H. & Okpeku, I. 2015 Production of activated carbon and characterization from snail shell waste (*Helix pomatia*). *Advances in Chemical Engineering and Science* **5**(1), 51–61.

Hao, G. & Xianlun, D. 2013 Preparation and characterization of activated carbon from palm shell by catalytic activation with steam. *Advanced Materials Research* **787**, 46–51.

Hasanzadeh, V., Rahmanian, O. & Heidari, M. 2020 Cefixime adsorption onto activated carbon prepared by dry thermochemical activation of date fruit residues. *Microchemical Journal* **152**, 104261.

Hock, P. E. & Zaini, M. A. A. 2018 Activated carbon by zinc chloride activation for dye removal – a commentary. *Acta Chimica Slovaca* **11**(2), 99–106.

Hui, T. S. & Zaini, M. A. A. 2015 Potassium hydroxide activation of activated carbon: a commentary. *Carbon Letters* **16**(4), 275–280.

Ismail, B., Hussain, S. T. & Akram, S. 2013 Adsorption of methylene blue onto spinel magnesium aluminate nanoparticles: adsorption isotherms, kinetic and thermodynamic studies. *Chemical Engineering Journal* **219**, 395–402.

Kang, S., Jiang, S., Peng, Z., Lu, Y., Guo, J., Li, J., Zeng, W. & Lin, X. 2018 Valorization of humins by phosphoric acid activation for activated carbon production. *Biomass Conversion and Biorefinery* **8**(4), 889–897.

Khamkeaw, A., Jongsomjit, B., Robison, J. & Phisalaphong, M. 2018 Activated carbon from bacterial cellulose as an effective adsorbent for removing dye from aqueous solution. *Separation Science and Technology* **54**(14), 2180–2193.

Kumar, A. & Jena, H. M. 2015 High surface area microporous activated carbons prepared from Fox nut (*Euryale ferox*) shell by zinc chloride activation. *Applied Surface Science* **356**, 753–761.

Laverde, M. P., Salamanca, M., Agredo, J. S., Losada, L. M. & Palma, R. A. T. 2019 Selective removal of Acetaminophen in urine with activated carbons from rice (*Oryza sativa*) and coffee (*Coffea arabica*) husk: effect of activating agent, activation temperature and analysis of physical-chemical interactions. *Journal of Environmental Chemical Engineering* **7**(5), 103318.

Lei, Y., Huang, R., Guo, L., Xie, H., Zhang, D. & Li, M. 2019 Effect of activating agents on the structure and capacitance performance of tofu derived porous carbon. *Journal of Materials Science: Materials in Electronics* **30**, 10274–10283.

Ma, H. T., Ho, V. T. T., Pham, N. B., Nguyen, D. C., Vo, K. T. D., Ly, H. C. & Tuan, P. D. 2017 Effect of the carbonization and activation process on the adsorption capacity of rice husk activated carbon. *Vietnam Journal of Science and Technology* **55**(4), 494–502.

Ma, R., Qin, X., Liu, Z. & Fu, Y. 2019 Adsorption property, kinetic and equilibrium studies of activated carbon fiber prepared from liquefied wood by $ZnCl_2$ activation. *Materials* **12**, 12091377.

Naga, A. O. A., Saied, E., Shaban, M. E., & Kady, S. A. & E, F. Y. 2019 Fast removal of diclofenac sodium from aqueous solution using sugar cane bagasse-derived activated carbon. *Journal of Molecular Liquids* **285**, 9–19.

Nahil, M. A. & Williams, P. T. 2012 Pore characteristics of activated carbons from the phosphoric acid chemical activation of cotton stalks. *Biomass and Bioenergy* **37**, 142–149.

Nandi, M., Okada, K., Dutta, A., Bhaumik, A., Maruyama, J., Derks, D. & Uyama, H. 2012 Unprecedented CO_2 uptake over highly porous N-doped activated carbon monoliths prepared by physical activation. *Chemical Communications* **48**, 10283–10285.

Nasrullah, A., Saad, B., Bhat, A. H., Khan, A. S., Danish, M., Isa, M. H. & Naeem, A. 2018 Mangosteen peel waste as a sustainable precursor for high surface area mesoporous activated carbon: characterization and application for methylene blue removal. *Journal of Cleaner Production* **211**, 1190–1200.

Oliveira, G., Calisto, V., Santos, S. M., Otero, M. & Esteves, V. I. 2018 Paper pulp-based adsorbents for the removal of pharmaceuticals from wastewater: a novel approach towards diversification. *Science of the Total Environment* **631–632**, 1018–1028.

Rangabhashiyam, S., Anu, N. & Selvaraju, N. 2013 Sequestration of dye from textile industry wastewater using agricultural waste products as adsorbents. *Journal of Environmental Chemical Engineering* **1**(4), 629–641.

Reza, R. A. & Ahmaruzzaman, M. 2015 Comparative study of waste derived adsorbents for sequestering methylene blue from aquatic environment. *Journal of Environmental Chemical Engineering* **3**(1), 395–404.

Saad, M. J., Chia, C. H., Zakaria, S., Sajab, M. S., Misran, S., Rahman, M. H. A. & Chin, S. X. 2019 Physical and chemical properties of the rice straw activated carbon produced from carbonization and KOH activation processes. *Sains Malaysiana* **48**(2), 385–391.

Sangachini, A. Z., Galangash, M. M., Younesi, H. & Nowrouzi, M. 2019 The feasibility of cost-effective manufacturing activated carbon derived from walnut shells for large-scale CO_2 capture. *Environmental Science and Pollution Research* **26**(26), 26542–26552.

Water Practice & Technology Vol 15 No 4
doi: 10.2166/wpt.2020.094

Saygili, H. & Saygili, G. A. 2019 Optimized preparation for bimodal porous carbon from lentil processing waste by microwave-assisted K_2CO_3 activation: spectroscopic characterization and dye decolorization activity. *Journal of Cleaner Production* **226**, 968–976.

Seo, S. W., Choi, Y. J., Kim, J. H., Cho, J. H., Lee, Y. & Im, J. S. 2019 Micropore-structured activated carbon prepared by waste PET/petroleum-based pitch. *Carbon Letters* **29**(4), 385–392.

Sesuk, T., Tammawat, P., Jivaganont, P., Somton, K., Limthongkul, P. & Kobsiriphat, W. 2019 Activated carbon derived from coconut coir pith as high performance supercapacitor electrode material. *Journal of Energy Storage* **25**, 100910.

Shen, Y. & Zhang, N. 2019 Facile synthesis of porous carbons from silica-rich rice husk char for volatile organic compounds (VOCs) sorption. *Bioresource Technology* **282**, 294–300.

Shen, Y., Zhang, N. & Fu, Y. 2019 Synthesis of high-performance hierarchically porous carbons from rice husk for sorption of phenol in the gas phase. *Journal of Environmental Management* **241**, 53–58.

Singh, G., Kim, I. Y., Lakhi, K. S., Srivastava, P., Naidu, R. & Vinu, A. 2017 Single step synthesis of activated bio-carbons with a high surface area and their excellent CO_2 adsorption capacity. *Carbon* **116**, 448–455.

Singh, J., Bhunia, H. & Basu, S. 2019 Adsorption of CO_2 on KOH activated carbon adsorbents: effect of different mass ratios. *Journal of Environmental Management* **250**, 109457.

Sutisna, Wibowo, E., Rokhmat, M., Rahman, D. Y., Murniati, R., Khairurrijal & Abdullah, M. 2017 Batik wastewater treatment using TiO_2 nanoparticles coated on the surface of plastic sheet. *Procedia Engineering* **170**, 78–83.

Tang, S. H. & Zaini, M. A. A. 2016 Malachite green adsorption by potassium salts-activated carbons derived from textile sludge: equilibrium, kinetics and thermodynamics studies. *Asia-Pacific Journal of Chemical Engineering* **12**(1), 159–172.

Valladares, C., Cruz, J. F., Matejova, L., Herrera, E., Gomez, M. M., Solis, J. L., Soukup, K., Solcova, O. & Cruz, G. J. F. 2019 Study of the adsorption of dyes employed in the food industry by activated carbon based on residual forestry. *Journal of Physics* **1173**(1), 012009.

Vunain, E., Houndedjihou, D., Monjerezi, M., Muleja, A. A. & Kodom, B. T. 2018 Adsorption, kinetics and equilibrium studies on removal of catechol and resorcinol from aqueous solution using low-cost activated carbon prepared from sunflower (*Helianthus annuus*) seed hull residues. *Water, Air and Soil Pollution* **229**(11), 366.

Wu, H., Chen, R., Du, H., Zhang, J., Shi, L., Qin, Y., Yue, L. & Wang, J. 2018 Synthesis of activated carbon from peanut shell as dye adsorbents for wastewater treatment. *Adsorption Science and Technology* **37**(1–2), 34–48.

Yang, K., Peng, J., Srinivasakannan, C., Zhang, L., Xia, H. & Duan, X. 2010 Preparation of high surface area activated carbon from coconut shells using microwave heating. *Bioresource Technology* **101**(15), 6163–6169.

Yang, B., Liu, Y., Liang, Q., Chen, M., Ma, L., Li, L., Liu, Q., Tu, W., Lan, D. & Chen, Y. 2019 Evaluation of activated carbon synthesized by one-stage and two-stage co-pyrolysis from sludge and coconut shell. *Ecotoxicology and Environmental Safety* **170**, 722–731.

Zaini, M. A. A. & Kamaruddin, M. J. 2013 Critical issues in microwave-assisted activated carbon preparation. *Journal of Analytical and Applied Pyrolysis* **101**, 238–241.

Zhang, H., Yan, Y. & Yang, L. 2008 Preparation of activated carbons from sawdust by chemical activation. *Adsorption Science and Technology* **26**(7), 533–543.

Zhang, T., Fan, L. T., Walawender, W. P., Fan, M., Bland, A. E., Zuo, T. & Collins, D. W. 2010 Hydrogen storage on carbon adsorbents: A review. In: *Environanotechnology*, 1st edn (Fan, M. ed.). Elsevier Inc., Amsterdam, the Netherlands, pp. 137–163.

Zhang, Y., Song, X., Zhang, P., Gao, H., Ou, C. & Kong, X. 2020 Production of activated carbons from four wastes via one-step activation and their applications in Pb^{2+} adsorption: insight of ash content. *Chemosphere* **245**, 125587.

Zhou, B., Gao, Q., Wang, H., Duan, E., Guo, B. & Zhu, N. 2012 Preparation, characterization, and phenol adsorption of activated carbons from oxytetracycline bacterial residue. *Journal of the Air and Waste Management Association* **62**(12), 1394–1402.

Zhou, J., Luo, A. & Zhao, Y. 2018 Preparation and characterisation of activated carbon from waste tea by physical activation using steam. *Journal of the Air and Waste Management Association* **68**(12), 1269–1277.